Short-term monocular deprivation boosts neural responsiveness to audio-visual events for the undeprived eye

Federici A.[1], Bernardi G.[1], Senna I.[2], Fantoni M.[1], Ernst M.O.[2], Ricciardi E.[1], Bottari D.[1]

[1] MoMiLab, IMT School for Advanced Studies Lucca, 55100 Lucca, Italy

[2] Applied Cognitive Psychology, Ulm University, 89081 Ulm, Germany

Abreviated title: Temporary MD boosts neural response to audiovisual events

Corresponding author: Alessandra Federici alessandra.federici@imtlucca.it

Conflict of interest statement: The authors declare no competing financial interests.

Acknowledgments: We would like to thank Cesare V. Parise for the helpful discussion and feedback regarding data analysis.

Abstract

A brief period of monocular deprivation (MD) in adults is known to induce short-term plasticity of the visual system. However, to what extent MD impacts beyond visual processing is unclear. Here, we investigated alterations of visual and audio-visual processing induced by MD measuring neural oscillations. Results revealed that MD modified neural activities associated with unimodal and multisensory processes in an eye-specific manner. Selectively for the Deprived eye, alpha activity was reduced within the first 150 ms of visual processing. Conversely, the response to audio-visual events was enhanced in the gamma range only for the Undeprived eye within 100-300 ms after stimulus onset. The analysis of gamma responses to unimodal auditory events clarified that MD elicited a crossmodal upweighting for the Undeprived eye. Source modeling suggested that the right parietal cortex played a major role in both visual and audio-visual MD effects. Notably, visual and audio-visual processing alterations emerged selectively for the induced (but not the evoked) component of the neural oscillations, indicating primary alterations in feedback connectivity. These findings support a model in which MD increases excitability for the Deprived eye and neural responsiveness to audio-visual and auditory events for the Undeprived eye. On the one hand, these results reveal the causal impact of MD on both unisensory and multisensory processes but with distinct frequency-specific profiles and, on the other hand, highlight the feedback nature of short-term neural plasticity. Overall this study shed light on the high flexibility and interdependence of the unimodal and multisensory functions.

Significance Statement

Whether and how a brief period of monocular deprivation impacts multisensory processing is unclear. Our data reveal that neural plasticity elicited by short-term MD affects both visual and audio-visual processing. The neural response to visual events was strengthened after deprivation only for the Deprived eye. Conversely, the neural response to audio-visual stimuli was enhanced only for the Undeprived eye. Neural oscillations in distinct frequency ranges underpinned the two effects revealing specific neural signatures and specific temporal scales. Finally, observed neural changes suggested the prominent role of feedback connectivity in adult short-term plasticity.

Introduction

While neuroplasticity of the visual system is maximal during development (Hubel and Wiesel, 1970; Hensch, 2005; Espinosa and Stryker, 2012; Levelt and Ḧubener, 2012; Reh et al., 2020), evidence

that a certain degree of plasticity is retained in the adult visual cortex has accumulated (Karmarkar and Dan, 2006; Spolidoro et al., 2009; Espinosa and Stryker, 2012; Hensch and Quinlan, 2018). Studies in adults employing psychophysics and neuroimaging methods showed that a brief period of MD, a pivotal model for testing the plasticity of the visual system, alters ocular balance by strengthening visual processing of the deprived eye (Castaldi et al., 2020). These functional changes reflect ocular dominance shifts in V1 in favor of the deprived eye (Lunghi et al., 2015a; Binda et al., 2018) and are supposedly driven by homeostatic plasticity (Lunghi et al., 2015b), the mechanism involved in preserving the cortical excitatory-inhibitory balance (Turrigiano, 2012).

Alterations induced by MD seem to impact beyond visual processing. At the behavioral level, short-term MD was found to affect the interplay between sensory modalities (Lo Verde et al., 2017; Opoku-Baah and Wallace, 2020). Results were consistent with decreased multisensory integration for the deprived eye in which the visual processing was strengthened and increased auditory weighting during audio-visual processing for the undeprived eye, in which visual processing was weakened. However, the neural correlates of the altered interplay between vision and audition following MD are lacking. To this end, we exploited the model of MD to elicit short-term plasticity and characterized specific functional changes to visual and audio-visual processes. Results are able to inform whether short-term plasticity in visual and audio-visual functions depend on different neural mechanisms.

Here, we combined psychophysical and electrophysiological approaches. The *sound-induced flash illusion* (Shams et al 2000, Hirst et al., 2020), in which the number of perceived flashes can be biased by the number of concurring beeps, was employed. To investigate the impact of MD on visual processing, we measured neural oscillations in response to a single flash before and after a deprivation phase. To determine the existence of an audio-visual MD effect, the analysis focused on neural oscillations elicited by the *fission* illusion in which a single flash is coupled with two beeps, and two flashes can be perceived (Shams et al., 2000).

Neural correlates associated with visual and audio-visual processing were characterized by their spectral, temporal, and spatial properties. Reflecting cycles of high and low neuronal excitability, neural oscillations reveal perceptual organization in both visual (Jensen et al., 2014; VanRullen, 2016) and multisensory analyses (Cooke et al., 2019; Lennert et al., 2021). We expected MD to induce changes in alpha activity, which is known to reflect levels of inhibition (Klimesch et al., 2007; Klimesch, 2012), and, thus, increase the visual system excitability for the deprived eye (Lunghi et al., 2015a). Moreover, we hypothesized MD to alter responses in the gamma range. Gamma activity was as well associated with excitatory-inhibitory balance (Jensen et al., 2010; 2012), and its modulation

was found to be involved in eliciting a perceptual fission illusion (Bhattacharya et al., 2002; Mishra et al., 2007; Lange et al., 2011, 2013; Balz et al., 2016).

Importantly, distinct components of neural oscillations characterize different types of processing according to the direction of information flow: while the evoked activity, which is phase-locked to the stimulation, has mainly been associated with feedforward processing (thalamo-cortical), the induced oscillatory activity, which is not phase-locked to the onset of the stimulus, has mainly been associated with feedback processing (cortico-cortical connectivity, Klimesch et al., 1998; Tallon-Baudry and Bertrand, 1999; Chen et al., 2012). Studies in humans and non-human animal models demonstrated that permanent sensory deprivation primarily affects induced oscillatory activity (Bottari et al., 2016; Yusuf et al., 2017; Bednaya et al., 2021). As homeostatic plasticity is an intrinsic feedback mechanism (Turrigiano and Nelson, 2004), we predicted to primarily observe changes in induced oscillatory activity following temporary MD. By investigating induced and evoked components of neural oscillations, we assessed whether induced activity alterations represent a unique signature of permanent sensory deprivation or also characterize short-term neuroplasticity. Finally, source modeling approaches were employed to address the neural sources of short-term plasticity effects.

Overall, this study aims to test whether and how a brief period of monocular visual experience in adulthood can affect the neural processing of multisensory audio-visual events.

Materials and Methods

Participants

The minimum sample size for the EEG analysis (participants included in the *main experiment*) was estimated through simulations. We used the procedure described in Wang and Zhang (2021; for details on sample size estimation, see Supplementary Materials Figure S1).

To determine individual suitability for the *main experiment*, potential participant completed a *preliminary behavioral assessment* (see the section below) in order to assess whether they meet the inclusion criteria: (i) to perceive the *fission illusion* with the dominant eye (>20% illusory rate), and (ii) to not be completely biased by the sound in the illusory conditions (>95% illusory rate). Out of twenty-seven young adults tested (mean age 28.22 ± 2.41 SD, twelve males) six participants were excluded as they did not meet these inclusion criteria or could not comply with the experimental instructions (see Supplementary Materials). Out of the 21 participants who performed the *main experiment*, one further participant was excluded due to his poor behavioral performance (the number

of errors was 3 SD above the group mean in the conditions in which only auditory stimuli were presented, i.e., the control conditions). The final sample included 20 young-adult participants (mean age 28.45 ± 2.67 SD, eight males and twelve female). They all had normal or corrected-to-normal vision (visual acuity ≥ 8/10) and did not report hearing deficits nor a history of neurological conditions. Since one EEG and one behavioral dataset, from different participants, went lost due to technical issues during acquisitions, the final sample included 19 behavioral and 19 EEG datasets. The study was approved by the local Ethical Committee (Comitato Etico di Area Vasta Nord Ovest Regione Toscana protocol n. 24579). Each participant signed a written informed consent before taking part in the experiment. The experimental protocol adhered to the principles of the Declaration of Helsinki (2013).

Stimuli and apparatus

The experiment was performed in a dimly lit and sound-attenuated chamber (BOXY, B-Beng s.r.l., Italy). Participants were comfortably sitting in front of the apparatus, with their eyes at a distance of 60 cm from the monitor. Visual stimuli were presented on an LCD monitor (60 Hz refresh rate; 24.5 inches; 1920 × 1080 screen resolution), and audio stimuli were delivered via a single speaker (Bose® Companion 2, series III multimedia) located below the screen and aligned with its center. Stimuli were flashes and beeps. Both visual and audio stimuli were created using Matlab (The Mathworks, Inc. - version 2017b). The audio stimulus was a 7 ms quadratic beep with a 3.5 kHz frequency and a sampling rate of 44.1 kHz, which was presented at about 75 dB. The visual stimulus was a 2° diameter grey dot displayed 5° below the center of the screen for 17 ms (corresponding to 1 frame) on a black background. The contrast level of the grey dot was selected individually via a staircase procedure to elicit the fission illusion in about 50% of trials (Pérez-Bellido et al., 2015, see below *Preliminary behavioral assessment*). Stimuli were delivered using E-Prime® software (version 2, Psychology Software Tools, Inc. www.pstnet.com). The Audio/Visual (AV) Device (Electrical Geodesics, Inc.) was employed to ensure accurate optimal synchronization between the presented stimuli and the recorded EEG traces.

Experimental Design

The whole procedure consisted of two main parts performed on two separate days: a *preliminary behavioral assessment* and the *main experiment*, in which the dominant eye was deprived of patterned visual input using a translucent eye patch. In both the *preliminary behavioral assessment* and the *main experiment,* participants performed a *monocular visual discrimination task*.

Monocular visual discrimination task

Participants were asked to report the number of perceived flashes (0, 1, or 2) while task-irrelevant beeps (0, 1, or 2) were presented. Responses were given by pressing one of three keypad buttons using the right-hand fingers. In each trial, audio (A) and visual (V) stimuli could be presented coupled or isolated constituting eight conditions: half the conditions were unisensory and comprised single or couples of visual or auditory events (visual: V and VV; auditory: A and AA) and the other half were multisensory (coherent audio-visual stimulation: AV and AVAV; illusory audio-visual stimulation: AVA and VAV, for a schematic summary of all conditions see the table reported in Figure 1a). Unisensory auditory trials (i.e., A and AA) represented control conditions. They were employed to ensure that participants correctly performed the task (participants with a number of errors 3 SD above the group mean were excluded from the analyses as described in Participants section). The presentation order of the conditions was randomized.

Since our main aim was to explore changes of the neural response to audio-visual events caused by a short-term MD, the main analysis focused on the audio-visual condition inducing fission illusion (AVA). Generating an unstable percept, this illusion allows investigating subtle changes in audio-visual processing. As a control, we investigated changes in the unisensory visual condition (V). Notably, in AVA and V conditions, the visual stimulus was the same single flash.

All trials started with a grey fixation cross presented at the center of the screen on a black background. After 717 ms, the stimulation was delivered. In the case of the fission illusion (i.e., AVA), each visual and auditory stimuli were separated by one frame (i.e., 17 ms; see an example for AVA condition in Figure 1a and Supplementary Materials). Following the stimulation, a blank screen appeared for 500 ms (response-free time window), then the fixation cross became white, and participants were asked to respond within 1 second (except for the staircase procedure, in which participants had infinite time to respond; see *Preliminary behavioral assessment*). As soon as the response was given, a blank screen was presented for 300 ms before the beginning of the subsequent trial. Participants were asked to maintain their gaze at the fixation cross throughout the duration of the trial.

Preliminary behavioral assessment

The ocular dominance via the Porta Test (see Supplementary Materials), the visual acuity via the eye chart, and the rate of the illusory percept during the *monocular visual discrimination task* were measured to verify if the participant could take part in the *main experiment*.

Once ocular dominance and visual acuity were tested, participants performed two short versions of the *monocular visual discrimination task*. The first short version comprised a staircase procedure (see Supplementary Materials for details) that was used to identify, at the individual level, the luminance

contrast between the grey dot and the black background, to elicit the fission illusion in about 50% of trials (Pérez-Bellido et al., 2015). Participants performed this test monocularly, with the dominant and non-dominant eye (the order was randomized). The contrast level for the dominant and non-dominant eye did not differ within-participant ($t(26)= -1.466$, $p=0.155$). The second short version of the *monocular visual discrimination task* (30 trials for each of the following conditions V, VV, AVA, VAV, A, and 6 for AA, AV, AVAV) was then performed with the dominant eye (with the contrast identified by the staircase procedure) to evaluate whether the participant was fulfilling the inclusion criteria to take part in the *main experiment* (see Participants section).

Previous evidence revealed that individual sensory preference (*Audio* or *Visual*) impacts on multisensory processing (Giard and Perronet, 1999). To assess whether individual sensory predisposition might affect multisensory short-term plasticity, participants monocularly performed a speeded object recognition task based on auditory, visual, and audio-visual information (see Supplementary Materials for details). Each participant's Sensory-Preference (*Audio* or *Visual*) was classified for each eye, and no significant difference was found between them ($p>0.68$). Sensory-Preference was an additional measure that we took into consideration: for this reason, the N within the *Audio* and *Visual* groups were not balanced.

Main experiment

Participants recruited in the *main experiment* came to the laboratory a second time on a different day. Since the *main experiment* lasted about five hours, the data were always acquired in the morning (approximately between 9 am and 2 pm) to avoid possible confounds associated with the circadian cycle or related to (visual) activities performed before the experiment. Each participant repeated the short version of the *monocular visual discrimination task* with the dominant eye comprising the staircase procedure to ensure the test-retest reliability of the selected visual stimulus contrast (no significant difference was found between the contrast levels measured in the two assessments; $t(20)=0.637$, $p=0.532$).

A brief practice of in total 16 trials was run before the *main experiment*. Participants performed the *monocular visual discrimination task*, with each eye, before (t0) and after (t1) a period of monocular deprivation (MD) (see Figure 1b), while their EEG signal was recorded. Thus, each participant performed a total of four sessions of the *monocular visual discrimination task* (i.e., at t0 and t1, both with the dominant and the non-dominant eye). Note that whether they started with the dominant or the non-dominant eye was counterbalanced across participants. MD consisted of 150 minutes in which the dominant eye was occluded by a translucent eye patch (Lunghi et al., 2011). From now on, we will refer to the dominant eye as the 'Deprived eye' and to the non-dominant eye as the

‘Undeprived eye’. To prompt active and controlled multisensory interactions with the environment during the MD phase, participants were engaged in predefined activities. Since the physical activity was demonstrated to boost short-term homeostatic plasticity in the adult visual cortex (Lunghi and Sale, 2015), all participants were engaged in the following activities: table football, table hockey, ping pong, and billiards, each of them lasting 15 minutes. The EEG cap was always kept on the scalp for the entire experiment duration.

Each monocular session (i.e., t0 Deprived, t0 Undeprived, t1 Deprived, and t1 Undeprived) comprised 100 trials for the conditions V, VV, AVA, VAV, A, and only 30 trials for the conditions AA, AV, AVAV, and was divided into five blocks (118 trials each) lasting about 5 minutes each. The number of trials was chosen to keep the duration of the monocular session within the estimated length of the MD effect (which has been demonstrated to be present for up to 90 minutes, but substantially decrease after 15 minutes; see Lunghi et al., 2011).

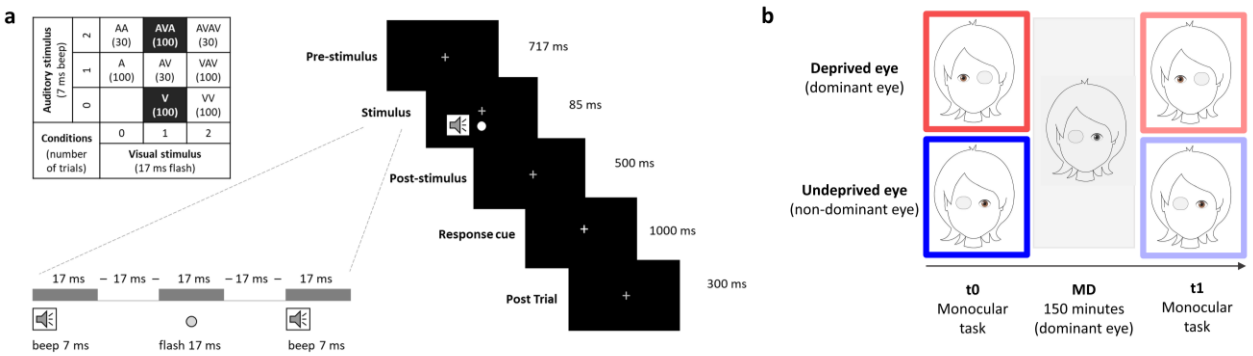

Figure 1. Schematic illustration of the experimental paradigm. (a) The top left table shows all the possible combinations of the stimuli (visual stimuli V and auditory stimuli A), representing all the eight possible conditions (conditions of interest are highlighted, and the number of trials in each condition is shown in brackets). On the right, an example of a single trial presentation in AVA condition is depicted. (b) Experimental procedure showing the four sessions performed with the Deprived eye (upper line, red contour) and the Undeprived eye (bottom line, blue contour). At t0 and t1, participants performed the visual monocular task with each eye (eye order was counterbalanced across participants). Between t0 and t1, participants wore a translucent eye patch on the dominant eye (Deprived eye) for 150 minutes (MD phase).

EEG recording and preprocessing

EEG data were collected continuously during the four monocular task sessions (i.e., t0 Deprived, t0 Undeprived, t1 Deprived, and t1 Undeprived), using Electrical Geodesics EEG system with 64-channels (EGI; 500 Hz sampling rate). Offline, the data of the four sessions were concatenated at the individual level to detect common stereotypical artifacts. Data were preprocessed implementing a validated approach (Stropahl et al., 2018; Bottari et al., 2020). The continuous recordings were

filtered (low-pass cut-off at 40 Hz, Hanning filter, order 500; high-pass cut-off at 1 Hz, Hanning filter, order 100) and downsampled to 250 Hz to reduce the computational time. The filtered and downsampled data were segmented into consecutive 1 second epochs and cleaned using joint probability criterion: segments displaying an activity with a joint probability across all channels larger than 3 SD were removed (Delorme et al., 2007). Independent Component Analysis (ICA) based on the extended Infomax (Bell and Sejnowski, 1995; Jung et al., 2000a, 2000b) was then performed. The resulting ICA weights were saved and applied to the raw continuous unfiltered data (Stropahl et al., 2018; Bottari et al., 2020). Components associated with stereotypical artifacts such as eye blinks and eye movements were identified and removed using a semiautomatic procedure (CORRMAP, Viola et al., 2009). The data were then low-pass and high-pass filtered (100 Hz, filter order 100; 0.1 Hz, filter order 500) with a Hanning filter. Noisy channels were identified based on visual inspection and then interpolated using spherical spline interpolation (mean interpolated electrodes per subject 2.32 ± 2.26 SD) and re-referenced to the average. Finally, the residual power line fluctuations at 50 Hz were removed using the CleanLine EEGlab plugin (https://github.com/sccn/cleanline). The EEG data were then split again into the original four sessions. Each session was then segmented into epochs of 2.2 seconds, from -1 to 1.2 seconds with respect to the onset of the stimulation. Noisy epochs were then rejected based on the joint probability across channels (Delorme et al., 2007) with a threshold of 3 SD (mean epochs rejected per subject 13% ± 4 SD). All these steps were performed with EEGLAB software (Delorme and Makeig, 2004). Data were then imported in Fieldtrip (Oostenveld et al., 2011) to perform time-frequency decomposition and statistical analyses.

Time-frequency decomposition

Time-frequency decomposition of the EEG data was performed within each session and separately for the visual and audio-visual conditions. Within each condition and session, we first extracted the induced power at a single trial level after subtracting the evoked activity (that is, subtracting from each trial the ERP computed averaging across trials without low-pass filtering). Time-frequency decomposition of single-trials was computed at each channel, separately for low (2-30 Hz) and high (30-80 Hz) frequency ranges. The oscillations in low frequencies were estimated using a Hanning taper with a frequency-dependent window length (4 cycles per time window) in steps of 2 Hz. Oscillations with higher frequencies were estimated using a Multitapers method with Slepian sequence as tapers, in steps of 5 Hz with a fixed-length time window of 0.2 seconds and fixed spectral smoothing of ± 10 Hz. For both frequency ranges, the power was extracted over the entire epoch (from -1 to 1.2 seconds) in steps of 0.02 seconds. Then, the average across trials was computed at the individual level within each session (t0 Deprived, t0 Undeprived, t1 Deprived, t1 Undeprived),

conditions (V and AVA), and frequency range (low and high). The resulting oscillatory activity was baseline-corrected to obtain the relative signal change with respect to the baseline interval. For the low-frequency range, the baseline was set between -0.7 and -0.3 seconds, while for the high-frequency range, it was between -0.2 and -0.1 seconds. The low-frequency range, having longer cycles, required a wide baseline for the appropriate estimation of slow oscillations, and was kept temporally distant from the stimulus onset to avoid temporal leakage of post-stimulus activity into the baseline period. The same procedure, without ERP subtraction from single trials, was implemented to estimate the total power. The baseline-corrected evoked power was computed by subtracting the baseline-corrected induced power from the baseline-corrected total power.

Source reconstruction

To better characterize the neural alterations induced by MD, source estimation of the neural effects was performed using Brainstorm software (Tadel et al., 2011) on preprocessed EEG data. Sources were extracted by applying a dynamic statistical parametric mapping (dSPM; Dale et al., 2000), adopting minimum-norm inverse maps to estimate the locations of scalp electrical activities. For each dataset, we used single trials pre-stimulus baseline [− 0.1 to 0.002 s] to calculate single subject noise covariance matrices and to estimate individual noise standard deviations at each location (Hansen et al., 2010). The boundary element method (BEM) provided in OpenMEEG was adopted as a head model; the model was computed on the first dataset and then applied to all the others (default parameters in Brainstorm were selected). Source estimation was performed by selecting the option of constrained dipole orientations (Tadel et al., 2011). Time-frequency decomposition was computed for each participant on the estimated sources at the single-trial level using the same approach described for the time-frequency decomposition performed at the sensor level.

Statistical analysis

Behavioral data

For each participant, we computed the d-prime (d') as visual and audio-visual sensitivity indices: d' = z(p hits) - z(p false alarms), where z is the inverse cumulative normal function, and p is the proportion of hits and of false alarms out of signal and noise, respectively. Values equal to 0 or 1 were corrected as 1/n and (n-1)/n, respectively, with n being the number of signal or noise trials. To compute the visual d', we defined as hits trials in which participants perceived one flash (V condition) and correctly responded 'one'. Consequently, false alarms were trials in which two flashes were presented (VV), and participants responded to having seen one flash. To compute the audio-visual

d', we defined, coherently with the fission illusion literature, false alarms AVA trials in which participants reported two flashes (Watkins et al., 2006; Whittingham et al., 2014; Pérez-Bellido et al., 2015; Vanes et al., 2016; Keil, 2020). Thus, AVAV trials in which participants correctly responded 'two flashes' were considered hits. Note that the audio-visual sensitivity (d') is inversely related to the amount of fission illusion: smaller d' indicated a greater amount of illusory percepts and vice-versa (note that Response means of each condition are reported in Supplementary Materials Figure S2).

Two mixed-design ANOVA, with Eye (Deprived and Undeprived) and Time (t1 and t0) as within-subjects factors, and Sensory-Preference (*Audio* and *Visual*) in the Deprived eye and Sensory-Preference (*Audio* and *Visual*) in the Undeprived eye as between-subjects factors, were performed separately on visual and audio-visual d' values. The Sensory-preference between-subjects factors were inserted in order to control their impact on the visual and audio-visual perception.

Neural oscillations

Oscillatory activity occurring after stimulus onset was analyzed separately for visual (V) and audio-visual (AVA) trials to assess MD impact on visual and audio-visual processing. Time-frequency analyses were separately performed for induced and evoked oscillatory activity for both low [4-30 Hz] and high [30-80 Hz] frequency ranges.

To assess the impact of MD, we subtracted the oscillatory activity recorded before MD from the oscillatory activity recorded after MD (i.e., t1 minus t0). This difference was computed separately for the Deprived and Undeprived eye. From now on, *PowChangeDeprived* represents relative changes in power due to MD for the Deprived eye, and *PowChangeUndeprived* the relative changes in power due to MD for the Undeprived eye.

To compare the impact of MD on Deprived and Undeprived eye, a series of non-parametric cluster-based permutation tests were performed via a paired-sample t-test, without a priori assumptions (i.e., across all electrodes, time-points, and frequencies) between *PowChangeDeprived* and *PowChangeUndeprived*. We used the Monte Carlo method with 1000 random permutations; cluster-level statistics were calculated taking the sum of the t-values within every cluster, with an alpha level of 0.05 (two-tailed) and a minimum neighbor channel = 1. Identified clusters were considered significant at $p<0.025$ (corresponding to a critical alpha level of 0.05 in a two-tailed test). We focused on the post-stimulus activity, and thus, statistical tests were performed for the entire response-free time window, that is, from 0 to 0.5 seconds. The time period after 0.5 seconds from the stimulation onset was discarded to prevent including motor artifacts. If a significant difference due to MD emerged in this test (*PowChangeDeprived* vs. *PowChangeUndeprived*), we assessed whether

differences between the two eyes emerged at t0 or t1. To this end, two planned comparisons (i.e., t0 Deprived vs. t0 Undeprived and t1 Deprived vs. t1 Undeprived) were performed using the same cluster-based permutation analysis approach and the same parameters reported above.

Correlations between neural and behavioral changes

Pearson correlations were employed to assess whether the neural changes related to short-term MD were associated with behavioral changes. When multiple correlations were performed to the same dataset, their results were compared employing a bootstrap method adapted for independent samples (see https://github.com/GRousselet/blog/tree/master/comp2dcorr).

Results

Behavioral data

Unisensory visual

The mixed-design ANOVA on visual d' with Eye (Deprived and Undeprived) and Time (t1 and t0) as within-subjects factors and Sensory-preference in the Deprived or in the Undeprived eye as between-subjects factor revealed a significant main effect of Time ($F(1,15)=13.52$, $p=0.002$), but no main effect of Eye, Sensory-Preference in the Deprived or in the Undeprived eye, nor other interaction effects were found (all *p*s>0.1). These findings suggest a general decrease of sensitivity at t1 (mean d' ± SE for each session: t0 Deprived 1.44 ± 0.21; t1 Deprived 1.13 ± 0.22; t0 Undeprived 1.37 ± 0.26; t1 Undeprived 1.14 ± 0.23; see Figure 2a).

Audio-visual

The mixed-design ANOVA performed on audio-visual d' revealed a significant main effect of Eye ($F(1,15)=7.53$, $p=0.015$), showing that the Undeprived eye was less susceptible to the fission illusion (mean d' ± SE for each session: t0 Deprived 0.58 ± 0.16; t1 Deprived 0.53 ± 0.19; t0 Undeprived 0.84 ± 0.23; t1 Undeprived 0.66 ± 0.17). A tendency towards significance emerged for the interaction between Eye, Sensory-Preference in the Deprived eye and Sensory-Preference in the Undeprived eye ($F(1,15)=4.01$; $p=0.064$). This tendency might suggest that participant's Sensory-Preference had an eye-specific impact; being an *Audio*-subject or a *Visual*-subject might affect the level of the fission illusion perceived with that eye (in Deprived eye mean d' ± SE A-group: 0.52 ms ± 0.19; V-group: 0.69 ms ± 0.20; in the Undeprived eye A-group: 0.65 ms ± 0.20; V-group: 0.96 ms ± 0.36). No significant main effect of Time, Sensory-Preference in the Deprived or in the Undeprived eye, nor other interactions emerged (all *p*s>0.08). Notably, a strong fission illusion was elicited in both eyes as highlighted by the small d' measured in each of the four sessions (see Figure 2b).

Since no main effect of the Sensory-Preference emerged neither in visual nor in audio-visual ANOVAs, the analyses of EEG activity were performed on the whole group.

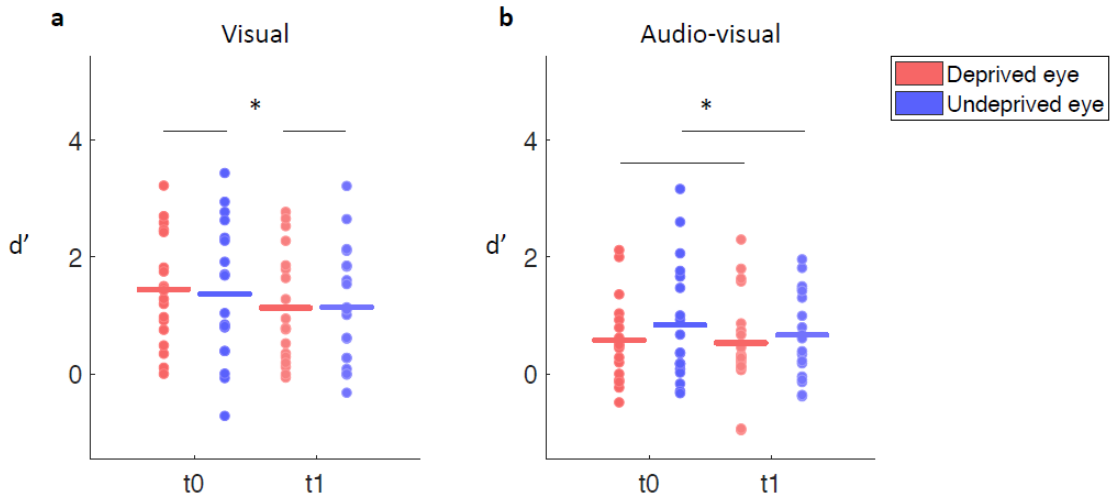

Figure 2. Behavioral performance computed as sensitivity (d'). (a) Both in visual and (b) audio-visual conditions, the group mean d' is reported for t0 and t1 within each eye (Deprived and Undeprived); superimposed dots represent single subjects' data; significant differences are highlighted with *. Sensitivity in the visual condition decreased after MD in both Deprived and Undeprived eye. Fission illusion in audio-visual condition was greater for the Deprived than Undeprived eye.

Neural oscillations

To specifically investigate whether MD primarily affected feedback and/or feedforward connectivity, we assessed the impact of MD on induced and evoked neural oscillations associated with the processing of visual and audio-visual stimuli.

Unisensory Visual

Induced power. The cluster-based permutation test performed on induced oscillatory activity within the low-frequency range [4-30 Hz] revealed a significant difference for *PowChangeDeprived* vs. *PowChangeUndeprived* ($p<0.009$) spanning from occipital to frontal regions. MD elicited a marked decrease of induced activity in the alpha range [10-16 Hz] between 0 to 0.12 seconds selectively for the Deprived eye (see Figure 3a, b). While no significant effects were found when comparing the oscillatory activity between the two eyes at t0 (all $ps>0.51$), the comparison performed on induced oscillatory activity measured at t1 revealed a significant difference ($p<0.002$) between Deprived and Undeprived eye for the power in the alpha range [10-16 Hz]. To further investigate the time-course of the MD effect in the alpha range, we tested the difference between t1 and t0 for each eye (i.e., Deprived, Undeprived). For each session and participant, the mean induced alpha power [10-16 Hz]

measured across three occipital electrodes (E36, E38, E40, which corresponded to the peak of the statistical effect in the *PowChangeDeprived* vs. *PowChangeUndeprived* cluster-based permutation test) was extracted. A series of paired t-tests were performed between t0 and t1 for each eye, at each time-point within the whole-time window of interest [0-0.5 s] (FDR corrected, q=0.05). A significant difference was found only for the Deprived eye (from 0 to 0.14 s; for Undeprived eye all ps>0.97; see Figure 3c).

No significant differences between *PowChangeDeprived* and *PowChangeUndeprived* were found in the high-frequency range [30-80 Hz] (all *ps*>0.67, see Figure S3).

Evoked power. Cluster-based permutation analyses on evoked oscillatory activity were performed contrasting *PowChangeDeprived* vs. *PowChangeUndeprived* to test whether MD alters feedforward visual processing. No significant differences emerged in either low or high frequencies (all *p*s>0.13, see Figure S4).

In sum, a visual MD effect emerged selectively for the Deprived eye and in the induced oscillatory activity within the alpha range.

Source analysis

We investigated the electrical sources of the visual MD effect. To this end, a permutation paired t-test (1000 randomizations) was performed at the source level, on the power in the alpha range [10-16 Hz] between t0 and t1 for the Deprived eye (time window [0-0.5 s]; FDR correction was applied on the time dimension). Results revealed that the visual MD effect was mainly located within the right hemisphere and comprised the superior parietal gyrus, the superior occipital gyrus, intraparietal and subparietal sulcus, and extend to calcarine sulcus (corrected p-threshold: 0.003; see Figure 3d).

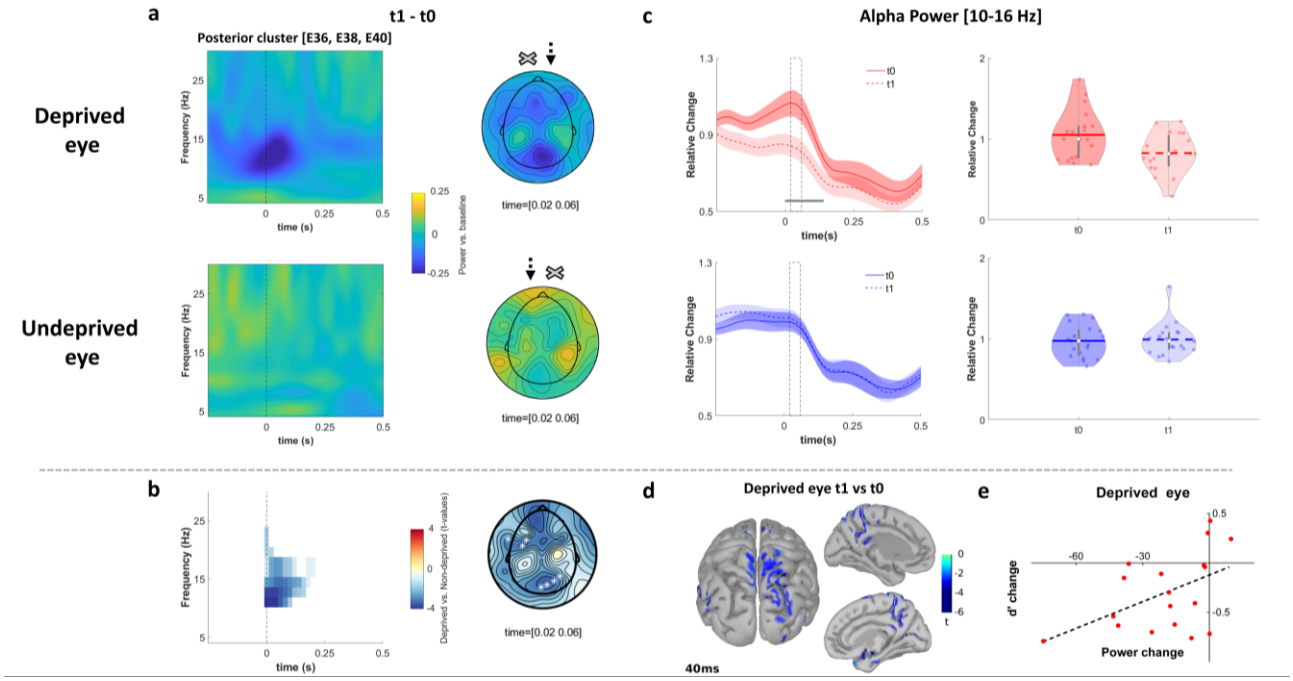

Figure 3. The effect of Monocular Deprivation (MD) on visual processing, visual MD effect. (a) Oscillatory activity calculated as the difference between t1 minus t0 at each eye: *PowChangeDeprived* (upper row) and *PowChangeUndeprived* (bottom row) are plotted as a function of time [-0.25 - 0.5 s] and frequency [4-30 Hz]. The plots show the average across occipital electrodes (E36, E38, E40); 0 s indicates stimulus onset. Topographies in the alpha range [10-16 Hz] at a representative time window [0.02 - 0.06 s]; arrows indicate which eye was stimulated (here depicted a participant with right-eye dominance), crosses represent the eye covered by a translucent patch. (b) Statistical results. Time-frequency plot highlighting significant differences between *PowChangeDeprived* and *PowChangeUndeprived* identified by the cluster-based permutation test ($p<0.025$, two-tailed) and the corresponding topography for the alpha range [10-16 Hz] at a representative time window [0.02 - 0.06 s]; electrodes belonging to the significant cluster are highlighted with white asterisks. (c) Time-course at the group level of the mean power in the alpha range [10-16 Hz] at t0 and t1 (data are averaged across electrodes E36, E38, E40) separately displayed for the Deprived and the Undeprived eye (upper and bottom rows); shaded areas represent the standard error of the mean; the continuous horizontal grey line indicates the significant difference between t0 and t1 in the Deprived eye (from 0 to 0.14 s; $p<0.05$, FDR corrected). The dashed grey boxes represent the time window [0.02 - 0.06 s], comprising the alpha peak, in which the power in the alpha range [10-16 Hz] was extracted for each subject (across channels E36, E38, E40) and shown in the corresponding violin plots (right side; each dot represents individual data). (d) Source analysis performed to localize the visual MD effect; the image shows at 40 ms after stimulus onset the area in which the power in the alpha range [10 - 16 Hz] significantly decreased at t1 with respect to t0. (e) The scatter plot shows, in the Deprived eye, individual change in visual sensitivity (d' change between t0 and t1 for the Deprived eye) as a function of alpha decrease (normalized *PowChangeDeprived* in the alpha range [10 - 16 Hz], within the time window [0.02 - 0.06 s], averaging across the E36, E38, E40 channels); the dashed line represents the linear correlation ($r(18) = 0.492$, $p=0.038$).

Audio-visual

After we assessed the impact of MD on unisensory visual processing (visual MD effect), we investigated whether MD can also affect audio-visual processing at the neural level. The induced and evoked oscillatory activities were tested separately within low and high-frequency ranges.

Induced power. The cluster-based permutation performed on induced oscillatory activity within the low-frequency range [4-30 Hz] between *PowChangeDeprived* and *PowChangeUndeprived* showed no significant effects (all ps>0.45, see Figure S5). In contrast, the same analysis performed within the high-frequency range [30-80 Hz] revealed a significant effect in gamma activity ($p<0.015$). An increase in gamma activity [65-75 Hz] was found in the Undeprived eye between 0.16 and 0.26 s, mainly in posterior electrodes (see Figure 4a, b). The planned comparison showed no significant effect at t0 (all ps>0.07), while a significant difference between the two eyes emerged only at t1 ($p<0.022$), confirming that MD specifically guided the effect. To further investigate the time-course of the induced gamma effect, we tested the difference between t0 and t1 within each eye. For each session and participant, the mean induced gamma power [65-75 Hz] measured across two parieto-occipital electrodes (E40 and E42, which corresponded to the peak of the statistical effect in the *PowChangeDeprived* vs. *PowChangeUndeprived* cluster-based permutation test) was extracted. A series of paired t-tests were performed between t0 and t1 for each eye, at each time-point within the whole-time window of interest [0-0.5 s] (FDR corrected, q=0.05). Only for the Undeprived eye a significant effect was found (from 0.12 to 0.2 s; for Deprived eye all ps>0.5; see Figure 4c).
The gamma band increase for audio-visual processing of the Undeprived eye following MD might suggest an upweighting of the auditory modality. If this would be the case, a greater neural response in the gamma range to unimodal acoustic stimulation (A and AA condition) should emerge selectively for the Undeprived eye after MD. A cluster-based permutation performed between t0 and t1 on induced oscillatory activity within the high-frequency range [30-80 Hz], across all electrodes and time-point [0-0.5s] confirmed this hypothesis (Undeprived eye $p<0.04$; conversely, no significant effect emerged for the Deprived eye all ps>0.35; see Supplementary Materials and Figure S6).

Evoked power. When the difference between *PowChangeDeprived* and *PowChangeUndeprived* was tested in the evoked power, no significant difference was found within the low-frequency range (all ps>0.09), nor within the high-frequency range ($p>0.05$, see Figure S7).

To sum up, the audio-visual MD effect selectively emerged for the Undeprived eye in the induced gamma power. This neurophysiological change seems to be driven by increased responsiveness to auditory inputs.

Source analysis

We investigated the sources of the audio-visual MD effect. To this end, a permutation paired t-test (1000 randomizations) was performed at the source level, on the power in the gamma range [65-75 Hz] between t0 and t1 for the Undeprived eye (time window [0-0.5 s]; FDR correction was applied on the time dimension).

Results revealed that audio-visual MD effect was mainly located at the cortical level around the right intraparietal sulcus and seems to comprise subcortical structures including the left thalamus (corrected p-threshold: 0.002; see Figure 4d). Despite localization of subcortical EEG activity should be take with caution, recent attempts showed that this is possible (Farahani et al., 2019). Importantly, the thalamus is a well known multisensory structure (Tyll et al., 2011; Froesel et al., 2021).

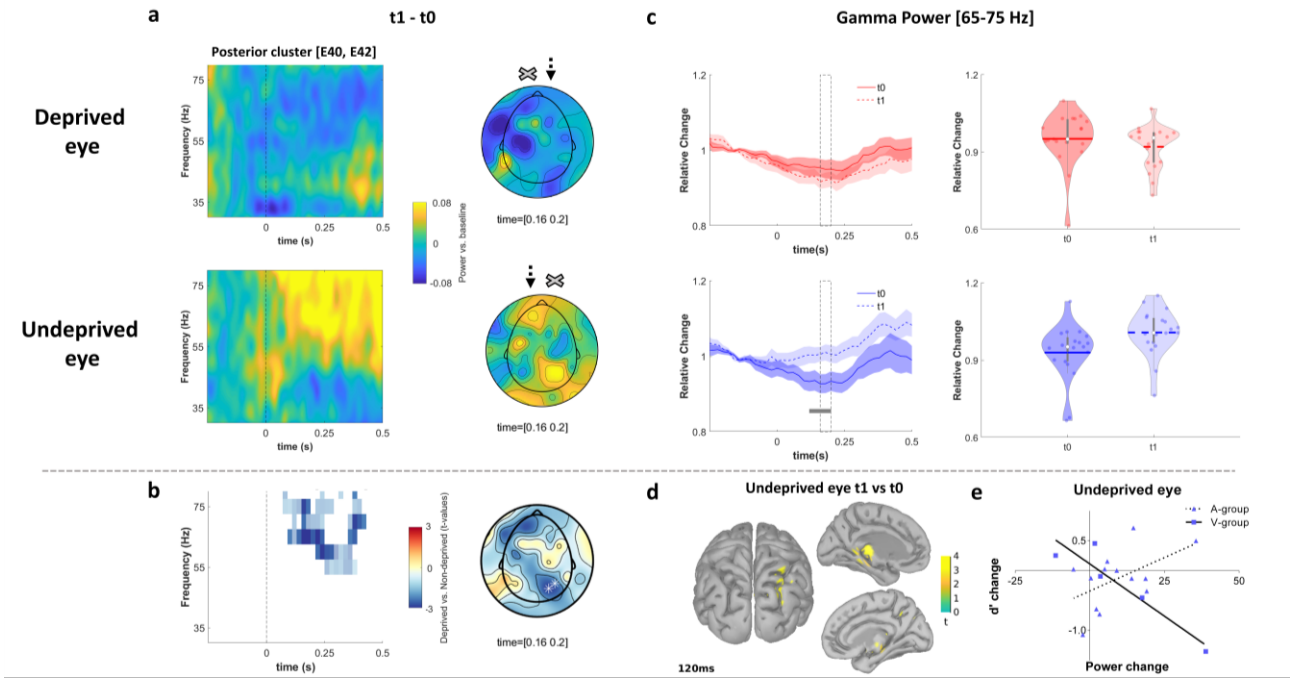

Figure 4. The effect of Monocular Deprivation (MD) on audio-visual processing, audio-visual MD effect. Oscillatory activity calculated as the difference between t1 minus t0 at each eye: *PowChangeDeprived* (upper row) and *PowChangeUndeprived* (middle row) are plotted as a function of time [-0.25 - 0.5 s] and frequency [30-80 Hz]. The plots show the average across posterior electrodes (E40, E42); 0 s indicates the stimulus onset. Topographies in the gamma range [65-75 Hz] at representative time window [0.16 - 0.2 s]; arrows indicate which eye was stimulated (represented in a participant with a right-eye dominance), and crosses represent the eye covered by a translucent patch. (b) Statistical results. Time-frequency plot highlighting significant differences between *PowChangeDeprived* and *PowChangeUndeprived* identified by the cluster-based permutation test ($p<0.025$, two-tailed) and corresponding topography for the gamma range [65-75 Hz] at a representative time window [0.16 - 0.2 s]; electrodes belonging to the significant cluster are highlighted with white asterisks. (c) Time-course at the group level of the mean power in gamma range [65-75 Hz] at t0 and t1 (data are averaged across electrodes E40, E42) separately displayed for the Deprived and the Undeprived eye (upper and bottom rows); shaded areas represent the standard error of the mean; the continuous

horizontal grey line indicates a significant difference between t0 and t1 for the Undeprived eye (from 0.12 to 0.2 s after stimulus onset; $p<0.05$, FDR corrected). The dashed grey boxes represent the time window [0.16 - 0.2 s] in which the power in the gamma range [65-75 Hz] was extracted for each subject (across channels E40 and E42) and shown in the corresponding violin plots (right side). (d) Source analysis performed to localize the audio-visual MD effect; the image shows at 120 ms after stimulus onset the area in which the power in the gamma range [65-75 Hz] significantly increases at t1 with respect to t0. (e) The scatter plot shows, in the Undeprived eye, individual change in audio-visual sensitivity (d' change between t0 and t1 for the Undeprived eye) as a function of gamma enhancement (normalized *PowChangeUndeprived* in the gamma range [65-75 Hz], within the time window [0.16-0.02 s], averaging across electrodes E40 and E42). Triangles represent *Audio*-subjects (A-group), while squares represent *Visual*-subjects (V-group); dotted and continued lines, indicate the two linear correlations for A-group ($r(13) = 0.513$; $p=0.073$) and V-group ($r(5) = -0.937$; $p=0.019$), respectively.

Association between neural and behavioral changes due to MD

For visual and audio-visual conditions, we investigated the degree of association between brain activity alterations and changes in behavioral performance. The average power at the frequencies of interest was extracted within a time window and across channels that resulted significant in the cluster-based permutation tests (visual and audio-visual MD effects). At the individual level, we computed the normalized difference between t1 and t0 within each eye ([*PowChangeDeprived/t0 Deprived*] * *100;* [*PowChangeUndeprived/t0 Undeprived*] * *100*). Within each condition (i.e., visual and audio-visual) and for each eye (i.e., Deprived and Undeprived), the power change was correlated (Pearson correlation) with the corresponding change in sensitivity between t0 and t1.

Unisensory Visual

We first tested whether observed changes of oscillatory activity in induced alpha power following MD (visual MD effect) were associated with changes in behavioral performance. To this aim, we extracted for each session the average power in the 10-16 Hz range between 0.02 and 0.06 s from the three significant electrodes (E36, E38, and E40). Then the normalized t1-t0 difference of *PowChangeDeprived* and *PowChangeUndeprived* was computed.

A significant positive correlation between normalized *PowChangeDeprived* and visual sensitivity change in the Deprived eye (d' change) was found ($r(18) = 0.492$, $p=0.038$). Following MD, the visual sensitivity in the Deprived eye decreased in parallel with a reduction in induced alpha power in the same eye (see Figure 3e). When the correlation between induced alpha change and visual sensitivity change was tested for the Undeprived eye, no significant effect was found ($p>0.99$).

Audio-visual

Next, we tested whether the increase in induced gamma after MD period (audio-visual MD effect) was associated with illusory fission percept. Thus, within each session, the induced power between 65 and 75 Hz was extracted within the 0.16-0.2 s time window and across the two significant posterior channels (E40 and E42). Then, the normalized t1-t0 difference of *PowChangeDeprived* and of *PowChangeUndeprived* was computed. No significant correlation was found neither for the Deprived eye nor for the Undeprived eye (all ps>0.43). However, at the behavioral level, a tendency between illusion perception and sensory preferences was found. Therefore, we additionally explored whether the association between neural and behavioral changes might be affected by the individual sensory preference: we assessed the correlation between *PowChangeUndeprived* and audio-visual d' change in the Undeprived eye, within *Audio* and *Visual* groups, classified according to participants' Sensory-Preference (estimated for the same eye). Pearson correlation revealed a significant negative correlation in the V-group (r(5) = -0.937; p=0.019), while a tendency toward a significant positive correlation was found in the A-group (r(13) = 0.513; p=0.073). The two correlations significantly differed (difference=1.45 CI [0.17 1.80], see Supplementary Materials Figure S8). These results suggest that the audio-visual MD effect might have a different impact on the illusory percept according to the participants' Sensory-Preference: in V-group, the increase of induced gamma activity in the Undeprived eye was positively associated with a fission illusion increase (smaller d' after MD), while in A-group the increase of induced gamma activity was associated with a fission illusion decrease (larger d' after MD).

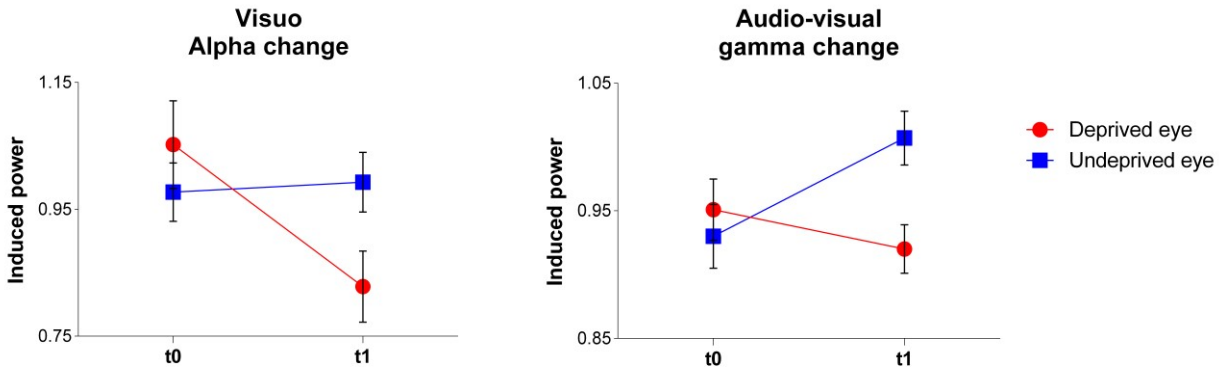

Figure 5. Visual and audio-visual MD effects on induced oscillatory activity. The plots show the % normalized power change due to MD in unisensory visual and multisensory audio-visual processing. On the left, the visual MD effect: decreased induced alpha power selectively for the Deprived eye (red) during unisensory visual processing. On the right, the audio-visual MD effect: enhanced induced gamma power selectively for the Undeprived eye (blu) during audio-visual processing. Each dot represents the group mean and bars the SE.

Discussion

In this study, adult neural plasticity of both unisensory visual and multisensory audio-visual processes was investigated to assess whether the impact of MD extends beyond visual processing. Induced and evoked oscillatory activity changes both in visual and audio-visual processing were measured after 150 minutes of altered visual experience (short-term MD). Induced alpha associated with the early phase of visual processing (<150ms) decreased after MD selectively for the Deprived eye. Conversely, induced gamma associated with audio-visual processing increased after MD only in the Undeprived eye, within a later temporal window (~100-300ms). Notably, both visual and audio-visual processing alterations were found selectively for the induced component of neural oscillations (see Figure 5). Source modeling linked the visual MD effect to the right parieto-occipital cortex and the audio-visual MD effect to the right intraparietal sulcus. Our data reveal the specific neural signatures of temporary MD effects on visual and audio-visual processes and shed light on their shared feedback nature. We demonstrated that a brief period of monocular visual experience in adulthood specifically changes the neural response to multisensory audio-visual events because of plasticity in feedback connectivity.

Spectro-temporal properties of the visual MD effect

The observed visual MD effect is in line with previous studies (Lunghi et al., 2015a, 2015b; Zhou et al., 2015; Binda et al., 2018; Schwenk et al., 2020). The reduced alpha activity observed when the task was performed with the Deprived eye after MD is consistent with increased excitability to compensate for the absence of stimulation during the deprivation phase. Source modeling suggested that the alpha reduction was mainly localized in the right hemisphere in superior parieto-occipital areas with some activities extending to primary visual areas (calcarine sulcus). These results confirm the modulation of alpha rhythm induced by short-term plasticity, previously shown as change in alpha peak amplitude (Lunghi et al., 2015a), and characterize the spectro-temporal properties of this neural effect. Namely, a selective decrease of alpha [10-16 Hz] occurs in the early stages of visual processing (<150ms). Notably, only induced activity (i.e., not phase-locked to stimulus onset) was altered by MD, revealing the feedback nature of visual short-term plasticity. Overall, these results are coherent with spectroscopy data showing an increase of excitability in the early visual cortex as indicated by reductions of inhibitory gamma-amino butyric acid (GABA) concentration after short-term MD (Lunghi et al., 2015b). Moreover, selectively for the Deprived eye, a significant correlation was found between the decrease in induced alpha activity and the decrease in visual sensitivity after MD,

suggesting a potential link between this neural change and the ability to discriminate temporal aspects of visual processing.

The impact of MD on audio-visual processing

Previous behavioral studies have shown that multisensory perception can be altered by MD (Lo Verde et al., 2017; Opoku-Baah and Wallace, 2020). By measuring changes in neural oscillations, we assessed neural mechanisms underpinning multisensory short-term plasticity and revealed the specific enhancement of induced gamma activity [65-75 Hz] selectively for the Undeprived eye when processing audio-visual input. The audio-visual MD effect involved the right intraparietal sulcus, suggesting its central role in short-term plasticity induced by MD.

We hypothesized that the audio-visual MD effect could be due to a crossmodal upweighting of the other modality (i.e., audition). To this end, we tested whether the neural response to unimodal auditory stimuli was increased following MD in each eye. The observation that gamma response to auditory input increased following MD selectively for the Underprived eye confirmed our hypothesis. This result revealed that short-term plasticity following MD alters both visual and auditory neural representations. Interestingly, alterations of neural excitability due to temporary binocular deprivation were previously shown to increase heteromodal responses in the visual cortex (Merabet et al., 2008). From a neurophysiological perspective, it is important to remark that neural profiles of short-term plasticity following MD seem to depend on the type of input at hand. While the visual stimulus was the same in visual and audio-visual conditions, short-term plasticity was characterized by specific oscillatory fingerprints (Siegel et al., 2012): alpha decreased during visual processing while gamma increased during audio-visual and auditory processing.

To what extent does this neural alteration interact with individuals' sensory predisposition? In the Undeprived eye, the correlation between enhanced gamma activity in audio-visual processing and behavioral performance showed opposite directions according to participants' Sensory-Preference. Gamma increased together with the illusory percept in *Visual*-subjects. Conversely, the opposite pattern was found in *Audio*-subjects, highlighting that the upweighting of auditory information during audio-visual processing after MD affects visual perception according to individual sensory preference. Coherently with the extreme flexibility and adaptability of multisensory functions (Giard and Perronet, 1999; Fujisaki et al., 2004; Van Atteveldt et al., 2014), the perception of the multisensory input after MD might change as a function of individual sensory predisposition. This inference could be further verified with psychophysics experiments (see Rohe et al., 2019) designed to directly estimate auditory modality's weight changes during audio-visual processing after MD.

Binocular input was shown to be critical for developing audio-visual perception: anomalies in different audio-visual perceptual tasks were reported in cases of monocular enucleation (Moro and Steeves, 2018a, 2018b), individuals affected by early monocular cataracts (Chen et al., 2017), and people suffering from amblyopia (Narinesingh et al., 2015, 2017; Richards et al., 2017). The present results, revealing that MD induces short-term plasticity of audio-visual processing, encourage possible treatments of audio-visual anomalies associated with MD. Increasing evidence in animal studies support clinical treatment of adult amblyopia (Hensch and Quinlan, 2018), and crucially a recent study conducted with adult people affected by amblyopia has shown that MD combined with physical exercise could be a promising clinical intervention to promote visual recovery (Lunghi et al., 2019). Future studies could be helpful to test whether multisensoryaudio-visual processing could also benefit from this novel clinical treatment.

The pivotal role of feedback connectivity in experience-dependent plasticity

Both visual and audio-visual MD effects were selectively found in induced neural oscillations, reflecting main alterations in feedback connectivity (Klimesch et al., 1998; Tallon-Baudry and Bertrand, 1999; Chen et al., 2012). Instead, the evoked activity (feedforward), likely revealing processing within the thalamo-cortical pathway, was not affected.

Visual MD effect was found in the induced alpha band, which was previously demonstrated to be drastically impaired by the transient absence of visual experience during development (Bottari et al., 2016). Animal studies involving congenital deaf cats demonstrated that induced and not evoked oscillatory activity in the auditory cortex is extremely reduced across a wide range of frequency bands (e.g., Yusuf et al., 2017). The authors hypothesized that the absence of sensory stimulation prevents the development of neural mechanisms allowing the integration of sensory signals and internal representations. Evidence of alterations of induced oscillatory activity following sensory deprivation was reported not only within modality, for visual (Bottari et al., 2016) and auditory systems (Yusuf et al., 2017), but also cross-modally. In humans, early-onset deafness selectively affects induced oscillatory activity associated with visual processing (Bednaya et al., 2021). The present audio-visual MD effect (increased induced gamma activity) provides evidence in the same direction also for multisensory processing. Taken together, this evidence suggests a substantial alteration of cortico-cortical feedback activities, in case of sensory input absence in both developmental and adult brain, for unisensory and multisensory functions. This is in line with previous evidence suggesting that the plasticity of feedback connectivity represents an extremely flexible mechanism to process sensory information according to changing demands (Polley et al., 2006).

Limitations of the study

Here, we focused on neural oscillations changes, and given the time constraints intrinsic in the MD effect (which is maximum within the first 15 minutes following the deprivation, Lunghi et al., 2011), we could not insert a direct measure of ocular dominance, which is usually assessed with binocular rivalry (e.g., Lunghi et al., 2011). Thus, we relied on eye-specific oscillatory activity alterations as proof of the change in interocular excitability balance: the strengthening of the Deprived eye after MD was demonstrated by the reduced alpha activity during visual processing selectively for that eye. While a clear reduction of strength for the Undeprived eye (i.e., increased alpha activity) did not emerge, this is in line with the literature: the strongest impact of MD is known to be on the Deprived eye, while the opposite effect on the Undeprived eye was found to be much smaller (Lunghi et al., 2015a; Binda et al., 2018) or even absent (Zhou et al., 2015).

Conclusions

These results demonstrated that a brief period of monocular visual experience in adulthood is able to change the neural response not only to visual stimuli but also to multisensory events. The data unveiled the spectral fingerprints of adult short-term plasticity induced by a brief period of MD for visual and audio-visual processing. We found enhanced excitability (i.e., decreased induced alpha activity) for the Deprived eye during early phase of visual processing, and we demonstrated the presence of neural alterations beyond the visual processing. Gamma activity associated with audio-visual processing was increased by MD at a later latency and only when the task was performed with the Undeprived eye. The analyses of responses to unimodal auditory input indicate an upweighting of sound input following MD, selectively for the Undeprived eye. Importantly, these distinct neural effects were selectively found in the induced neural oscillations, revealing that experience-dependent plasticity mainly involves alterations in feedback connectivity not only during development but also in adulthood. This observation is consistent with the existence of a general mechanism shared across sensory modalities and across the life cycle.

References

Balz J, Keil J, Roa Romero Y, Mekle R, Schubert F, Aydin S, Ittermann B, Gallinat J, Senkowski D (2016) GABA concentration in superior temporal sulcus predicts gamma power and perception in the sound-induced flash illusion. Neuroimage 125:724–730

Bednaya E, Pavani F, Ricciardi E, Pietrini P, Bottari D (2021) Oscillatory signatures of Repetition Suppression and Novelty Detection reveal altered induced visual responses in early deafness. Cortex.

Bell AJ, Sejnowski TJ (1995) An information-maximization approach to blind separation and blind deconvolution. Neural Comput 7:1129–1159.

Bhattacharya J, Shams L, Shimojo S (2002) Sound-induced illusory flash perception: Role of gamma band responses. Neuroreport 13:1727–1730.

Binda P, Kurzawski JW, Lunghi C, Biagi L, Tosetti M, Morrone MC (2018) Response to short-term deprivation of the human adult visual cortex measured with 7T bold. Elife 7:1–25.

Bottari D, Bednaya E, Dormal G, Villwock A, Dzhelyova M, Grin K, Pietrini P, Ricciardi E, Rossion B, Röder B (2020) EEG frequency-tagging demonstrates increased left hemispheric involvement and crossmodal plasticity for face processing in congenitally deaf signers. Neuroimage 223:117315.

Bottari D, Troje NF, Ley P, Hense M, Kekunnaya R, Röder B (2016) Sight restoration after congenital blindness does not reinstate alpha oscillatory activity in humans. Sci Rep 6.

Castaldi E, Lunghi C, Morrone MC (2020) Neuroplasticity in adult human visual cortex. Neurosci Biobehav Rev 112:542–552.

Chen CC, Kiebel SJ, Kilner JM, Ward NS, Stephan KE, Wang WJ, Friston KJ (2012) A dynamic causal model for evoked and induced responses. Neuroimage 59:340–348.

Chen YC, Lewis TL, Shore DI, Maurer D (2017) Early Binocular Input Is Critical for Development of Audiovisual but Not Visuotactile Simultaneity Perception. Curr Biol 27:583–589.

Cooke J, Poch C, Gillmeister H, Costantini M, Romei V (2019) Oscillatory properties of functional connections between sensory areas mediate cross-modal illusory perception. J Neurosci 39:5711–5718.

Dale AM, Liu AK, Fischl BR, Buckner RL, Belliveau JW, Lewine JD, Halgren E (2000) Dynamic statistical parametric mapping: combining fMRI and MEG for high-resolution imaging of cortical activity. Neuron 26:55–67.

Delorme A, Makeig S (2004) EEGLAB: An open source toolbox for analysis of single-trial EEG dynamics including independent component analysis. J Neurosci Methods 134:9–21.

Delorme A, Sejnowski T, Makeig S (2007) Enhanced detection of artifacts in EEG data using

718 higher-order statistics and independent component analysis. Neuroimage 34:1443–1449.

719 Espinosa JS, Stryker MP (2012) Development and Plasticity of the Primary Visual Cortex. Neuron
720 75:230–249.

721 Farahani ED, Wouters J, van Wieringen A (2019). Contributions of non-primary cortical sources to
722 auditory temporal processing. NeuroImage, 191: 303-314.

723 Froesel M, Cappe C, Ben Hamed S (2021) A multisensory perspective onto primate pulvinar
724 functions. Neurosci Biobehav Rev 125:231–243.

725 Fujisaki W, Shimojo S, Kashino M, Nishida S (2004) Recalibration of audiovisual simultaneity. Nat
726 Neurosci 2004 77 7:773–778.

727 Giard MH, Peronnet F (1999). Auditory-visual integration during multimodal object recognition in
728 humans: a behavioral and electrophysiological study. Journal of cognitive neuroscience,
729 11:473-490.

730 Hansen P, Kringelbach M, Salmelin R (2010) MEG: An Introduction to Methods. Oxford
731 University Press (OUP).

732 Hensch TK (2005) Critical period plasticity in local cortical circuits. Nat Rev Neurosci 6:877–888.

733 Hensch TK, Quinlan EM (2018) Critical periods in amblyopia. Vis Neurosci 35:E014.

734 Hirst RJ, McGovern DP, Setti A, Shams L, Newell FN (2020) What you see is what you hear:
735 Twenty years of research using the Sound-Induced Flash Illusion. Neurosci Biobehav Rev
736 118:759–774.

737 Hubel DH, Wiesel TN (1970) The period of susceptibility to the physiological effects of unilateral
738 eye closure in kittens. J Physiol 206:419–436.

739 Jensen O, Bonnefond M, VanRullen R (2012) An oscillatory mechanism for prioritizing salient
740 unattended stimuli. Trends Cogn Sci 16:200–206.

741 Jensen O, Gips B, Bergmann TO, Bonnefond M (2014) Temporal coding organized by coupled
742 alpha and gamma oscillations prioritize visual processing. Trends Neurosci 37:357–369.

743 Jensen O, Mazaheri A (2010). Shaping functional architecture by oscillatory alpha activity: gating
744 by inhibition. Frontiers in human neuroscience, 186.

745 Jung T-P, Makeig S, Humphries C, Lee T-W, McKeown MJ, Iragui V, Sejnowski TJ (2000a)
746 Removing electroencephalographic artifacts by blind source separation. Psychophysiology

37:163–178.

Jung TP, Makeig S, Westerfield M, Townsend J, Courchesne E, Sejnowski TJ (2000b) Removal of eye activity artifacts from visual event-related potentials in normal and clinical subjects. Clin Neurophysiol 111:1745–1758.

Karmarkar UR, Dan Y (2006) Experience-dependent plasticity in adult visual cortex. Neuron 52:577–585.

Keil J (2020) Double Flash Illusions: Current Findings and Future Directions. Front Neurosci 14:1–8.

Klimesch W (2012) Alpha-band oscillations, attention, and controlled access to stored information. Trends Cogn Sci 16:606–617.

Klimesch W, Russegger H, Doppelmayr M, Pachinger T (1998) A method for the calculation of induced band power: Implications for the significance of brain oscillations. Electroencephalogr Clin Neurophysiol 108:123–130.

Klimesch W, Sauseng P, Hanslmayr S (2007) EEG alpha oscillations: The inhibition-timing hypothesis. Brain Res Rev 53:63–88.

Lange J, Oostenveld R, Fries P (2011) Perception of the touch-induced visual double-flash illusion correlates with changes of rhythmic neuronal activity in human visual and somatosensory areas. Neuroimage 54:1395–1405.

Lange J, Oostenveld R, Fries P (2013) Reduced Occipital Alpha Power Indexes Enhanced Excitability Rather than Improved Visual Perception. J Neurosci 33:3212–3220.

Lennert T, Samiee S, Baillet S (2021) Coupled oscillations enable rapid temporal recalibration to audiovisual asynchrony. Commun Bio, 4:1-12.

Levelt CN, Ḧubener M (2012) Critical-period plasticity in the visual cortex. Annu Rev Neurosci 35:309–330.

Lo Verde L, Morrone MC, Lunghi C (2017) Early Cross-modal Plasticity in Adults. J Cogn Neurosci 29:520–529.

Lunghi C, Berchicci M, Morrone MC, Di Russo F (2015a) Short-term monocular deprivation alters early components of visual evoked potentials. J Physiol 593:4361–4372.

Lunghi C, Burr DC, Morrone C (2011) Brief periods of monocular deprivation disrupt ocular

balance in human adult visual cortex. Curr Biol 21:538–539.

Lunghi C, Emir UE, Morrone MC, Bridge H (2015b) Short-Term monocular deprivation alters GABA in the adult human visual cortex. Curr Biol 25:1496–1501.

Lunghi C, Sale A (2015) A cycling lane for brain rewiring. Curr Biol 25:R1122–R1123.

Lunghi C, Sframeli AT, Lepri A, Lepri M, Lisi D, Sale A, Morrone MC (2019) A new counterintuitive training for adult amblyopia. Ann Clin Transl Neurol 6:274–284.

Merabet LB, Hamilton R, Schlaug G, Swisher JD, Kiriakopoulos ET, Pitskel NB, Kauffman T, Pascual-Leone A (2008). Rapid and reversible recruitment of early visual cortex for touch. PLoS one, 3:e3046.

Mishra J, Martinez A, Sejnowski TJ, Hillyard SA (2007) Early cross-modal interactions in auditory and visual cortex underlie a sound-induced visual illusion. J Neurosci 27:4120–4131.

Moro SS, Steeves JKE (2018a) Normal temporal binding window but no sound-induced flash illusion in people with one eye. Exp Brain Res 236:1825–1834.

Moro SS, Steeves JKE (2018b) Audiovisual plasticity following early abnormal visual experience: Reduced McGurk effect in people with one eye. Neurosci Lett 672:103–107.

Narinesingh C, Goltz HC, Raashid RA rha., Wong AMF (2015) Developmental Trajectory of McGurk Effect Susceptibility in Children and Adults With Amblyopia. Invest Ophthalmol Vis Sci 56:2107–2113.

Narinesingh C, Goltz HC, Wong AMF (2017) Temporal binding window of the sound-induced flash illusion in amblyopia. Investig Ophthalmol Vis Sci 58:1442–1448.

Oostenveld R, Fries P, Maris E, Schoffelen JM (2011) FieldTrip: Open source software for advanced analysis of MEG, EEG, and invasive electrophysiological data. Comput Intell Neurosci 2011.

Opoku-Baah C, Wallace MT (2020) Brief period of monocular deprivation drives changes in audiovisual temporal perception. J Vis 20:1–13.

Pérez-Bellido A, Ernst MO, Soto-Faraco S, López-Moliner J (2015) Visual limitations shape audio-visual integration. J Vis 15:1–15.

Polley DB, Steinberg EE, Merzenich MM (2006). Perceptual learning directs auditory cortical map reorganization through top-down influences. Journal of neuroscience, 26:4970-4982.

Reh RK, Dias BG, Nelson CA, Kaufer D, Werker JF, Kolbh B, Levine JD, Hensch TK (2020) Critical period regulation acrossmultiple timescales. Proc Natl Acad Sci U S A 117:23242–23251.

Richards MD, Goltz HC, Wong AMF (2017) Alterations in audiovisual simultaneity perception in amblyopia. PLoS One 12:1–20.

Rohe T, Ehlis AC, Noppeney U. (2019). The neural dynamics of hierarchical Bayesian causal inference in multisensory perception. Nature Communications, 10:1-17.

Schwenk JCB, VanRullen R, Bremmer F (2020) Dynamics of Visual Perceptual Echoes Following Short-Term Visual Deprivation. Cereb Cortex Commun 1:1–11.

Shams L, Kamitani Y, Shimojo S (2000) What You See Is What You Hear. Nature 408:2000.

Siegel M, Donner TH, Engel AK (2012) Spectral fingerprints of large-scale neuronal interactions. Nat Rev Neurosci 13:121–134.

Spolidoro M, Sale A, Berardi N, Maffei L (2009) Plasticity in the adult brain: Lessons from the visual system. Exp Brain Res 192:335–341.

Stropahl M, Bauer AKR, Debener S, Bleichner MG (2018) Source-Modeling auditory processes of EEG data using EEGLAB and brainstorm. Front Neurosci 12:1–11.

Tadel F, Baillet S, Mosher JC, Pantazis D, Leahy RM (2011) Brainstorm: A user-friendly application for MEG/EEG analysis. Comput Intell Neurosci 2011.

Tallon-Baudry C, Bertrand O (1999) Oscillatory gamma activity in humans and its role in object representation. Trends Cogn Sci 3:151–162.

Turrigiano G (2012) Homeostatic synaptic plasticity: Local and global mechanisms for stabilizing neuronal function. Cold Spring Harb Perspect Biol 4.

Turrigiano GG, Nelson SB (2004). Homeostatic plasticity in the developing nervous system. Nature reviews neuroscience, 5:97-107.

Tyll S, Budinger E, Noesselt T (2011) Thalamic influences on multisensory integration. Commun Integr Biol 4:378–381.

Van Atteveldt N, Murray MM, Thut G, Schroeder CE (2014) Multisensory integration: Flexible use of general operations. Neuron 81:1240–1253.

Vanes LD, White TP, Wigton RL, Joyce D, Collier T, Shergill SS (2016) Reduced susceptibility to

the sound-induced flash fusion illusion in schizophrenia. Psychiatry Res 245:58–65.

VanRullen R (2016) Perceptual Cycles. Trends Cogn Sci 20:723–735.

Viola FC, Thorne J, Edmonds B, Schneider T, Eichele T, Debener S (2009) Semi-automatic identification of independent components representing EEG artifact. Clin Neurophysiol 120:868–877.

Watkins S, Shams L, Tanaka S, Haynes JD, Rees G (2006) Sound alters activity in human V1 in association with illusory visual perception. Neuroimage 31:1247–1256.

Whittingham KM, McDonald JS, Clifford CWG (2014) Synesthetes show normal sound-induced flash fission and fusion illusions. Vision Res 105:1–9.

Yusuf PA, Hubka P, Tillein J, Kral A (2017) Induced cortical responses require developmental sensory experience. Brain 140:3153–3165.

Zhou J, Baker DH, Simard M, Saint-Amour D, Hess RF (2015) Short-term monocular patching boosts the patched eye's response in visual cortex. Restor Neurol Neurosci 33:381–387.

Supplementary Materials

Simple size estimation for the main EEG experiment

We estimated the minimum sample size needed to replicate previous evidence of neural MD effect on visual processing. Starting from the previous electrophysiological (EEG) studies (Lunghi et al., 2015a), we expected the effect to be in the alpha range [8-14 Hz], in the first stages of the visual processing [0-120 ms], and in occipito-parietal electrodes (E33, E34, E36, E38). Using the data of four pilot subjects, through simulations suited for cluster-based permutation tests (500 randomization; Wang and Zhang, 2021), we estimated a minimum sample size of 17 subjects to reach a power of 0.8 (lower threshold). Here, the final sample comprised 19 behavioral and 19 EEG datasets.

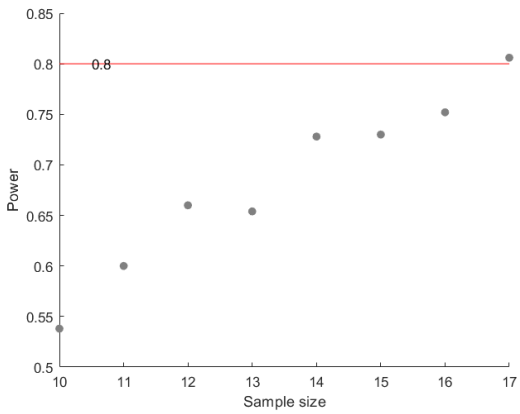

Figure S1. Sample Size Estimation. Expected statistical power at each sample size, starting from N=10, computed through simulations of time-frequency data on the total power (alpha= 0.05). Results showed that to achieve a power of 0.8 (red line) a minimum sample size of N=17 was required.

Participants excluded after the preliminary behavioral assessment

Five participants were excluded as they did not meet the inclusion criteria of the study: one perceived the fission illusion only in a few trials (20% illusory rate), and the other were entirely biased by the sound on their visual perception (>95% illusory rate). Moreover, one participant was excluded because they could not comply with instructions (difficulties in responding within the response time window).

Conditions trials

In fission illusion (AVA condition), the visual stimulus was presented between the two auditory stimuli, with the inter-stimulus-interval (ISI) between each stimulus being a single frame (i.e., 17 ms). The same was done for fusion illusion (VAV condition): the audio stimulus was presented within the two visual stimuli (ISIs between the stimuli: 17 ms). Instead, in coherent multisensory conditions (i.e., AV and AVAV), each audio-visual couple was presented simultaneously. In the AVAV condition, the two couples of stimuli were presented with an ISI of 51 ms (that corresponds to three frames, 17 ms × 3), as in the conditions with two unisensory stimuli (i.e., VV, AA).

Porta Test

To assess participant's eye dominance we used the Porta test. Participant extends one arm and with both eyes open aligns the thumb finger with a distant object. Then participant alternates closing the eyes, when the thumb appears to "move" it means that the closed eye is the dominant one (https://web.archive.org/web/20080215220943/http://www.sportvue.com/support/dominance.php).

Staircase procedure on the AVA condition

The contrast level of the grey dot presented on the screen was selected for each individual via a one-up one-down staircase procedure. In the staircase procedure, 133 contrasts for the grey dots were implemented (linearly spaced). When the subject's response corresponded to the perception of the fission illusion (i.e., response "two flashes"), the contrast decreased, while it increased after a non-illusion perception (i.e., response "one fash"). Wrong answers (i.e., response zero flashes) were not taken into account by the staircase procedure, and the same contrast was displayed again in the subsequent AVA trial. AVA condition trials were presented randomly with all the other conditions (i.e., A, AA, V, VV, VAV, AV, AVAV; maximum 15 trials for each condition). No more than three consecutive AVA trials could be displayed for a maximum of 99 trials. Flash contrast was randomly selected between 10 pre-selected contrasts in all the other conditions. The staircase procedure was considered completed when 16 reverses, changes of direction in the staircase, were reached. The threshold contrast value was computed as the mean of the last three levels of contrast that caused a reverse.

Speeded object recognition task

The speeded object recognition task was performed monocularly with the dominant (Deprived) eye and the non-dominant (Undeprived) eye in a randomized order.
We created two different objects: one was characterized by a small circle (1.7° diameter grey dot) and a high pitch sound (quadratic beep with a 3.8 kHz frequency and a sampling rate of 44.1 kHz). While the other by a bigger circle (2° diameter grey dot) and a lower pitch sound (quadratic beep with a 3.5 kHz frequency and a sampling rate of 44.1 kHz). The visual and auditory features were coupled in accordance with previously reported crossmodal correspondences between auditory pitch and size of visual objects (see review Spence, 2011). In each trial, participants were presented with one of the two objects defined either by visual feature alone (unisensory visual condition), auditory feature alone (unisensory auditory condition), or by the combination of auditory and visual features, and they were asked to recognize as soon as possible which of the two objects was presented. Twenty trials for each condition (only audio, only video, audio-visuo × 2 objects) were randomly presented. Computing the

median reaction times (RTs) at the single-subject level, only on correct trials and excluding the outliers above or below 3 SD from the median of each condition, we compared RTs in unisensory visual and unisensory auditory trials to define the Sensory-Preference of each participant. Subjects with shorter RTs in unisensory visual trials were considered *Visual* while those who were faster in unisensory auditory trials were considered *Audio*.

Behavioral results in all conditions

We reported here the mean of responses in each condition for each session. In all four sessions, we found an expected performance: when zero stimuli were presented, the means were close to zero, and the mean response increased when the number of the visual stimuli increased (maximal when 2 Visual and 2 Auditory stimuli were presented); participants are clearly able to perform the task in all sessions. Notably, the fission illusion was elicited in all sessions; indeed, AVA cell (1 Visual and 2 Auditory stimuli) is always whiter than AV cell (1 Visual and 1 Auditory stimulus).

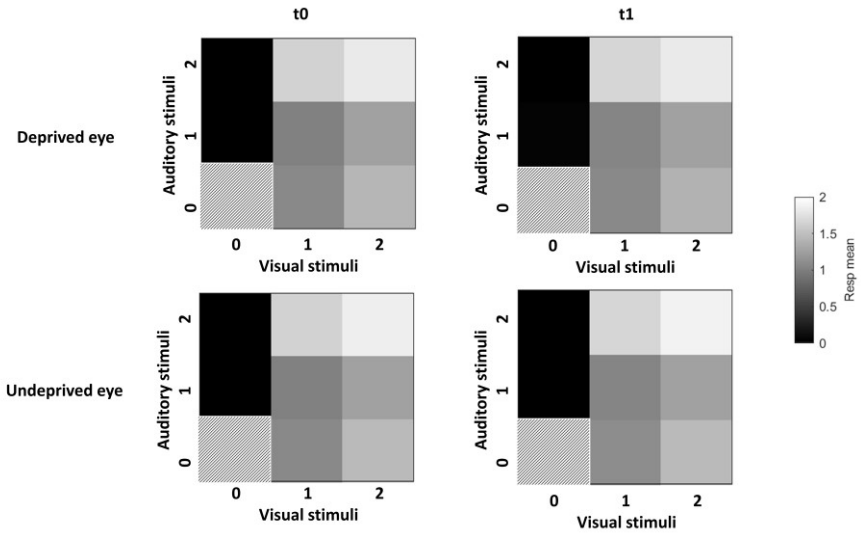

Figure S2. **Mean of response for each condition in each session.** The heatmaps of the four sessions (t0 Deprived, t0 Undeprived, t1 Deprived, t1 Undeprived) are shown at the group level. Each square represents one of the eight possible conditions, according to the stimulations delivered (the condition zero-zero is absent in our experiment, for this reason, we fill this square up with dashed lines). The color code represents the mean responses: black = zero is the minimum, and white = two is the maximum.

Unisensory visual

Induced power. No significant differences between *PowChangeDeprived* and *PowChangeUndeprived* were found in the high-frequency range (all ps>0.6).

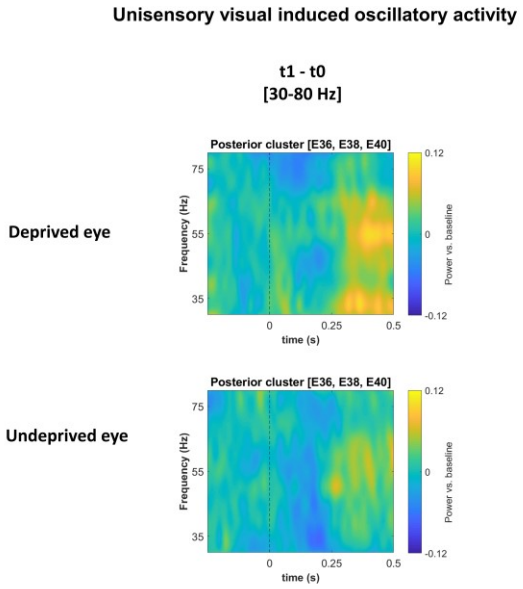

Figure S3. **Time-frequency plots showing high-frequency induced oscillatory activity during visual processing.** Oscillatory activity, calculated as the difference between t1 and t0 at each eye (upper row, *PowChangeDeprived*, t1 minus t0 at the Deprived eye, and bottom row, *PowChangeUndeprived*, t1 minus t0 at the Undeprived eye), are plotted as a function of time [-0.25 - 0.5 s] and frequency [30-80 Hz]. The data represent the average across occipital electrodes (E36, E38, E40); the dashed line at 0 s indicates the stimulus onset.

Evoked power. No significant differences emerged in either low or high frequencies (all *p*s>0.13).

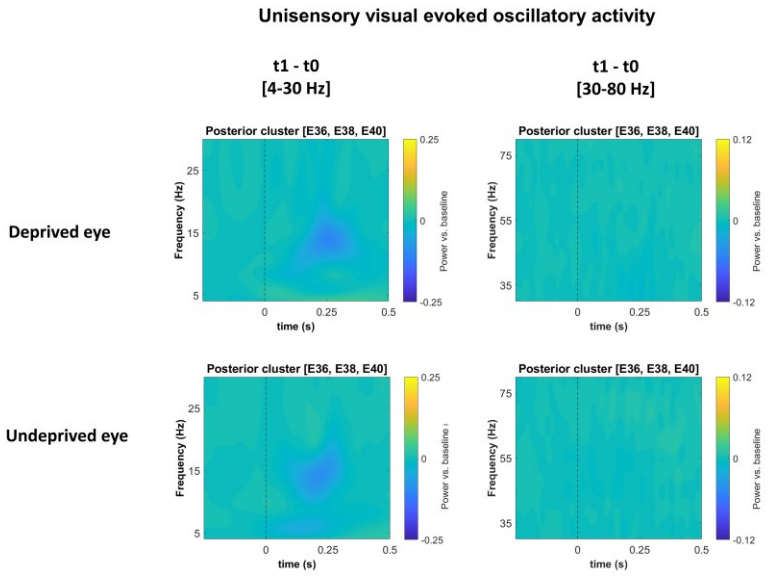

Figure S4. Time-frequency plots showing evoked oscillatory activity during visual processing. Oscillatory activity, calculated as the difference between t1 and t0 at each eye (upper row, *PowChangeDeprived*, t1 minus t0 at the Deprived eye and bottom row, *PowChangeUndeprived*, t1 minus t0 at the Undeprived eye), are plotted as a function of time [-0.25 - 0.5 s] and frequency [4-30 Hz] and [30-80 Hz] (left and right column, respectively). The data represent the average across occipital electrodes (E36, E38, E40); the dashed line at 0 s indicates the stimulus onset.

Audio-visual

Induced power. The cluster-based permutation performed between *PowChangeDeprived* and *PowChangeUndeprived* within the low-frequency range showed no significant effects (all *ps*>0.45).

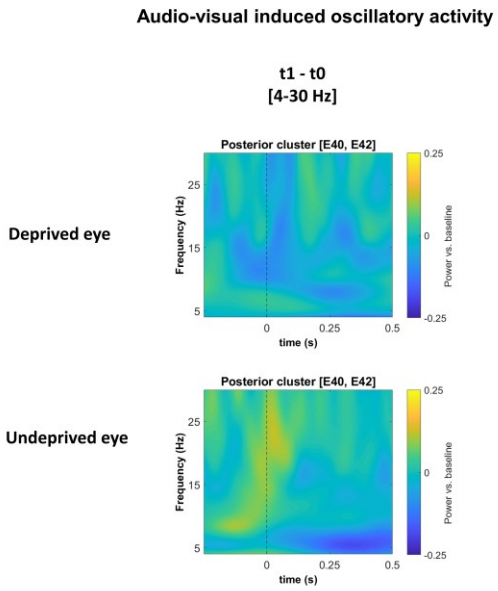

Figure S5. **Time-frequency plots showing low-frequency induced oscillatory activity during audio-visual processing.** Oscillatory activity, calculated as the difference between t1 and t0 at each eye (upper row, *PowChangeDeprived*, t1 minus t0 at the Deprived eye and bottom row, *PowChangeUndeprived*, t1 minus t0 at the Undeprived eye), are plotted as a function of time [-0.25 - 0.5 s] and frequency [4-30 Hz]. The data represent the average across two posterior electrodes (E40, E42); the dashed line at 0 s indicates the stimulus onset.

Response to unisensory auditory stimuli

A hypothesis-driven cluster-based permutation was performed to assess whether the gamma band increase for audio-visual processing of the Undeprived eye following MD is due to an upweighting of the auditory modality. To this end, a cluster-based permutation analysis on the induced oscillatory activity in the high-frequency range [30-80 Hz] ($p<0.05$ one tail) was performed across all electrodes, all frequencies, and within the whole-time window [0-0.5 s] between t0 and t1 in both eyes. The analysis revealed a significant increase in gamma activity between 100 and 300 ms in response to auditory stimulation after MD ($p<0.04$) selectively for the Undeprived eye. Conversely, no significant difference emerged for the Deprived eye ($p>0.35$).

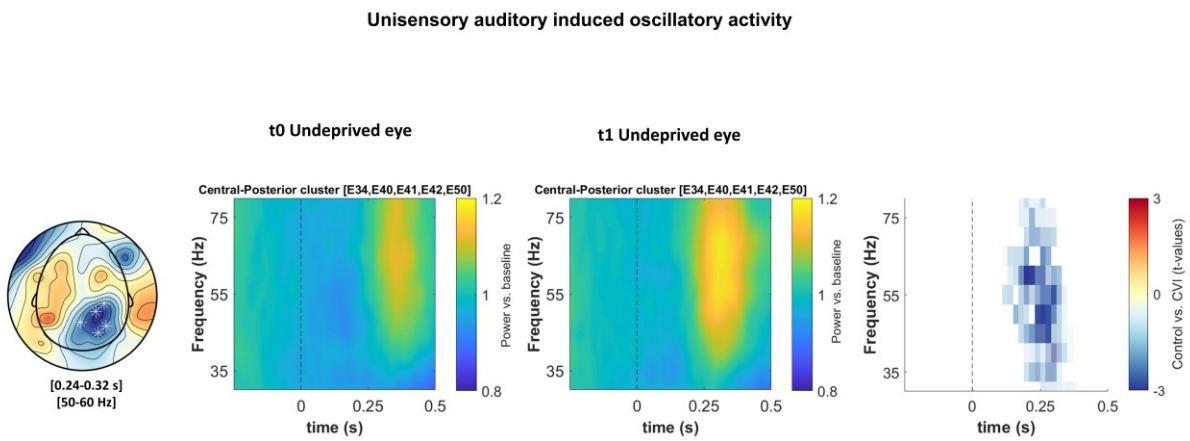

Figure S6 Increased induced gamma activity after MD during unisensory auditory processing for the Undeprived eye. Topography on the left side shows the results of statistics in the gamma range [50-60 Hz] over a representative time window [0.24 - 0.32 s]. White asterisks highlight significant electrodes (E34, E40, E41, E42, E50). The oscillatory activity averaged across significant electrodes are shown in the time-frequency plots at t0 and t1, plotted as a function of time [-0.25 - 0.5 s] and frequency [30-80 Hz]; on the right side, time-frequency plot highlighting significant differences between t0 and t1.

Evoked power. When we tested the difference between *PowChangeDeprived* and *PowChangeUndeprived* in the evoked power, no significant difference was found within the low-frequency range (all ps>0.09) nor within the high-frequency range (p>0.05).

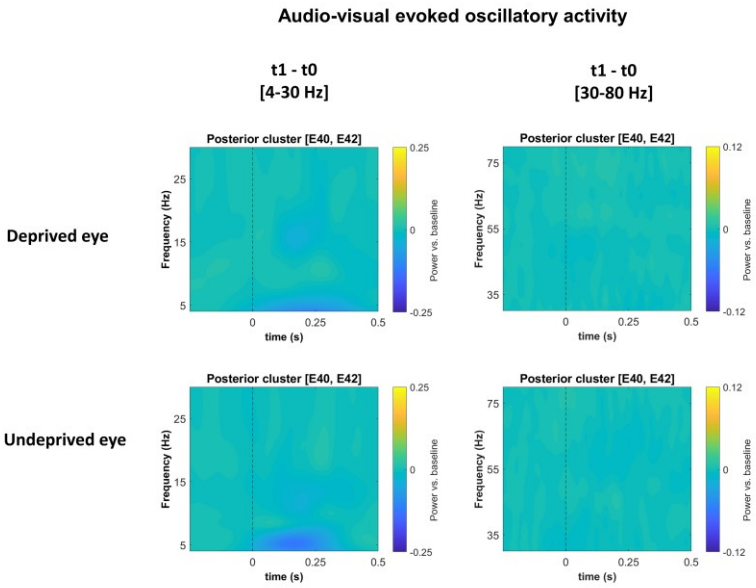

Figure S7. **Time-frequency plots showing evoked oscillatory activity during audio-visual processing.** Oscillatory activity, calculated as the difference between t1 and t0 at each eye (upper row, *PowChangeDeprived*, t1 minus t0 at the Deprived eye and bottom row, *PowChangeUndeprived*, t1 minus t0 at the Undeprived eye), are plotted as a function of time [-0.25 - 0.5 s] and frequency [4-30 Hz] and [30-80 Hz] (left and right column, respectively). The data represent the average across two posterior electrodes (E40, E42); the dashed line at 0 s indicates the stimulus onset.

Comparison between correlations in the audio-visual condition

After computing for A- and V- groups the correlations between normalized *PowChangeUndeprived* and d' change for the audio-visual condition in the Undeprived eye, we tested by means of the bootstrap method (Pernet, Wilcox & Rousselet, 2012) whether the difference between the two correlations was significantly different from zero. Since Pearson correlations were performed, the confidence interval was adjusted as described in Wilcox (2009).

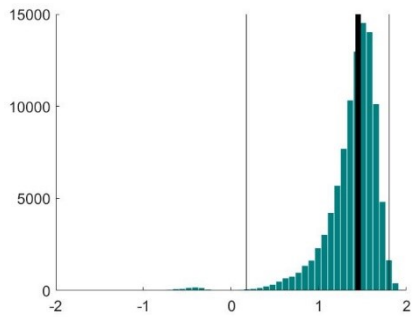

Figure S8. **Difference between correlations in the *Audio* and *Visual* groups**. The graph shows the distribution of the differences between correlations in the A- and V-groups (i.e., rA minus rV), computed by the bootstrap methods with

100000 repetitions. The thick black line is the difference between our correlations (rA-rV=1.45), and the thin lines indicate the CI [0.17 1.87].

References

Pernet CR, Wilcox RR, Rousselet GA (2013). Robust correlation analyses: false positive and power validation using a new open source matlab toolbox. Frontiers in psychology, 606.

Spence C (2011). Crossmodal correspondences: A tutorial review. Attention, Perception, & Psychophysics, 73(4): 971-995.Wang C, Zhang Q (2021). Word frequency effect in written production: Evidence from ERPs and neural oscillations. Psychophysiology, 58:e13775.